

Development of a Multi-channel Dispersion Interferometer at TEXTOR^a

A. Lizunov, P. Bagryansky, A. Khilchenko, Yu.V.Kovalenko, and A. Solomakhin

Budker Institute of Nuclear Physics, Novosibirsk 630090, Russia

W. Biel, H. T. Lambertz, Yu. Krasikov, M. Mitri, B. Schweer

Forschungszentrum Jülich GmbH, Association EURATOM-FZ Jülich, Institut für

Plasmaphysik, Trilateral Euregio Cluster, 52425 Jülich, Germany

H.Dreier

Max-Planck-Institut für Plasmaphysik, EURATOM Association, Wendelsteinstrasse 1,

D-17491 Greifswald, Germany

The design and main characteristics of fourteen-channel dispersion interferometer for plasma profile measurement and control in TEXTOR tokamak are presented. The diagnostic is engineered on the basis of modular concept, the 10.6 μm CO₂ laser source and all optical and mechanical elements of each module are arranged in a compact housing. A set of mirrors and retro-reflectors inside the TEXTOR vacuum vessel provides full coverage of the torus cross-section with twelve vertical and two diagonal

^a Contributed paper, published as part of the Proceedings of the 17th Topical Conference on High-Temperature Plasma Diagnostics, Albuquerque, New Mexico, May 2008

lines of sight, no rigid frame for vibration isolation is required. Results of testing of the single-channel prototype diagnostic and the pilot module of the multi-channel dispersion interferometer are presented.

01.30.Cc

I. INTRODUCTION

Interferometry is a widely known approach to measure line-integrated electron density in various plasma study applications. Different types of interferometers are being used nowadays in most plasma magnetic confinement devices like tokamaks, RFPs or mirror systems. Besides delivery of physical measurement information, interferometers are also applied to provide machine control functions like feedback signals to manipulate plasma density and position. Traditionally, interferometers with spatial separation of measurement channels are more common at fusion installations. However, these set-ups have several intrinsic disadvantages like sensitivity to vibrations and other sources of the measurement arm length instability. Additionally, the use of massive vibration isolation structures encompassing the plasma volume to reduce influence of vibration is not always possible in modern tokamaks. Among other solutions to overcome the above mentioned problem, two interferometer schemes are widespread:

- Interferometers using far-infrared radiation (118 μm , 337 μm) [1]
- Two-color interferometers [2,3].

As a third approach, a dispersion interferometer (DI), also “second harmonics interferometer” [4], utilizes the same principle as for a two-color interferometer, namely, separation of probing beams in frequency. The essential distinctive feature is that the second probing beam is generated by partial conversion of the first (or fundamental)

wave into second harmonic in a frequency doubler nonlinear crystal. Both fundamental (FH) and second harmonic (SH) waves propagate through the same path by the nature of SH generation. In the ideal case, the dispersion interferometer is only sensitive to the phase shift gained by the two waves in a medium. For plasma dispersion equation, this phase shift can be expressed as

$$\Delta\Theta = \frac{3e^2}{8\pi\epsilon_0 mc^2} \lambda \langle n_e l \rangle ;$$

here λ is the FH wavelength and $\langle n_e l \rangle$ the line integrated electron density.

Since no reference arm is necessary in a DI approach, one can make the diagnostic design relatively compact with all optical elements arranged on a single breadboard. This solution was implemented in the single-channel DI [5] for TEXTOR tokamak. This development work served as the basis for a multi-channel dispersion interferometer using a CO₂ continuous wave laser. The primary aims and performance characteristic of the multi-channel dispersion interferometer for TEXTOR are:

- 14 viewing lines (12 vertical and 2 diagonal);
- Measurement of plasma density spatial profile;
- Real-time control of the plasma density as well as the horizontal and vertical plasma position;
- Development and validation of techniques consistent with “next step” devices for fusion experiments like Wendelstein 7-X and ITER.

II. OPTICAL AND MECHANICAL DESIGN

II.1 SINGLE-CHANNEL MODULE

The projected multi-channel dispersion interferometer has a modular design, which offers high flexibility in diagnostic deployment and configuration and also enables one to interchange different interferometer modules. The main challenge in the realization of a **Single Module of Dispersion Interferometer (SIMDI)** is the development of a compact and robust optical and mechanical design ensuring vibration compensation for the optical elements along the line of sight. An additional boundary condition is the limited space reserved for the multi-channel DI at TEXTOR. Central element of the SIMDI is a horizontally mounted solid aluminum breadboard, elements of the SIMDI are arranged on both sides of its breadboard as shown in Fig.1 and 2. The interferometer module is based on the continuous wave 10.6 μm CO₂ laser; this choice is stipulated by successful application of a similar laser in the DI prototype diagnostic [5] at TEXTOR. The second reason for the choice of this particular wavelength is that the influence of refraction is negligible for 10.6 μm radiation and TEXTOR plasma parameters. At the same time the sensitivity is high enough. Beam splitters (4) and (12) in Fig. 1 reflect a small portion of the FH radiation to the laser power monitor (13) for a continuous control of the CO₂ source status. Two lenses (8) and (10) form a telescope with an aperture (9) in the beam waist: These elements provide a spatial separation of the probing and the backward beam to avoid undesirable additional interferometric effects. The periscope (11) reflects the probing beam by 90° to the “optical level”, where receiver is periscope head (1) in Fig. 2. The key SIMDI element is the frequency doubler crystal (3) in Fig. 2, where partial conversion of the primary radiation with $\lambda=10.6 \mu\text{m}$ into SH with $\lambda=5.3 \mu\text{m}$ takes place.

Unlikely the prototype DI [5], where ZnGeP_2 (ZGP) nonlinear crystal was used, an AgGaSe_2 (AGSE) crystal was chosen for the SIMDI. The main advantage of the new crystal is a negligible absorption at both wavelengths comparing to ZGP, where the absorption coefficient is approximately 0.8 cm^{-1} ($\lambda=9.6 \text{ }\mu\text{m}$). Additionally, an extensive study [6] shows several advantages of an AGSE for second harmonics generation: reasonable level of surface damage threshold and higher efficiency for wavelength $\lambda=10.6 \text{ }\mu\text{m}$. After passing the plasma volume, probing beam hollow corner cube retro-reflector mounted inside the TEXTOR vacuum vessel, the reflected backward beam is slightly vertically shifted. This allows the separation of the backward beam from the original one at mirror (2) in Fig. 2, where the upper half of the mirror is cut off. Numerical simulations have been used to pre-calculate the optimal beams characteristics, according to these calculations, the focal lengths of spherical mirrors (2), (4) and (7) were chosen.

Element (5) is an electro-optical cell based on a GaAs crystal; application of voltage $U=U_0 \cdot \sin(\Omega t)$, (where $U_0 \approx 4 \text{ kV}$, $\Omega=250 \text{ kHz}$) leads to the beam phase sweep $-\pi.. \pi$. The measurement technique based on the phase modulation (close to the well known zebra stripes method) is described in [5]. The periscope head (13) in Fig. 2 receives the He-Ne beam ($\lambda=0.63 \text{ }\mu\text{m}$), the plane mirror (6) is equipped with a small hole in the center to align the He-Ne beam with the CO_2 beam.

After separation at half-mirror (2), the backward beam is focused to the main photodetector (12). The photodetector uses a sapphire filter transparent for the $5.3 \text{ }\mu\text{m}$ wavelength but absorbing the remaining $10.6 \text{ }\mu\text{m}$ beam fraction. Thus, the interference signal produced by two SH waves, is analyzed. In addition, the mirror (11) contains four

small (1.5×1.5 mm) thermopile sensors arranged in a rectangular pattern. Measuring the position of the backward beam, these sensors are used for continuous monitoring of the status of in-vessel beam formation optics.

II.2 DESIGN OF MULTI-CHANNEL SYSTEM

The general views of design of the multi-channel dispersion interferometer are shown in Fig. 3 (derived from the 3-dimensional model of the diagnostic). The diagnostic contains fourteen modules (SIMDI) and allows to measure the line-integrated plasma density along fourteen chords as shown in Fig. 3. Twelve lines of sight (6) are vertically aligned and nearly uniformly distributed in the torus cross section. In addition to the estimation of the electron density profile, this configuration will be used for the detection of horizontal plasma displacements. Two additional diagonal lines of sight (7) are projected to register vertical plasma displacements.

II.3 CONTROL AND DATA ACQUISITION SYSTEM

The control and data processing system of the 14-channel DI consists of two independent but interacting segments. All “standard” control functions and the monitoring of the SIMDI status signals are realized on the base of an industrial SIEMENS S7-300 controller at each module. This solution is consistent with modular structure of the diagnostic and permits easy integration into existing TEXTOR control system framework. The subsystem responsible for data acquisition is developed specially for the multi-channel DI. Each SIMDI hosts the data processing electronic module based on a Programmable Logic Matrix (PLM) core. Usage of a PLM for signal processing enables a guaranteed real-time rate of output <nl> values calculation, this approach also gives flexibility to change programmed calculation algorithms. The real-time data processing

module delivers output signal via the serial fiber line to the remote signal conditioning rack connected to TEXTOR engineering systems controlling gas-puff valves and correction magnetic coils. All input/output channels of the diagnostic operate synchronously with the time frame of 4 μ s, which defines the maximal temporal resolution of measurements.

III. FIRST RESULTS

The proposed measurement and data conditioning approach was tested on the single-channel DI prototype in TEXTOR experiment. Fig. 4 shows line-integrated density plot obtained by this diagnostic in TEXTOR shot #104337. In this shot plasma density control was maintained by the dispersion interferometer. Plot in Fig. 5 also shows the signal measured by existing HCN interferometer-polarimeter at TEXTOR. In this particular experiment, the latter diagnostic experienced a fringe jump resulting from a fast change in the electron density, while dispersion interferometer worked normally. Fig. 5 demonstrates the sample of a $\langle n \rangle$ plot acquired during the recent commissioning session of the pilot SIMDI dedicated for the new multi-channel system.

ACKNOWLEDGEMENTS

The authors wish to thank the TEXTOR team for the kind and helpful support.

REFERENCES

- [1] H. R. Koslowski and H. Soltwisch, *Fusion Engineering and Design* **34-35** (1997) 143-150

- [2] T. Kondoh, A. E. Costley, T. Sugie, Y. Kawano, A. Malaquias, and C. I. Walker, *Review of Scientific Instruments*, **75** (2004) 3420.
- [3] K. Tanaka, A. L. Sanin, L. N. Vyacheslavov, T. Akiyama, K. Kawahata, T. Tokuzawa, Y. Ito, and S. Okajima, *Review of Scientific Instruments*, **75** (2004) 3429-3432.
- [4] F. C. Jobs and N. L. Bretz, *Review of Scientific Instruments* **68** (1997), 709-712
- [5] P. A. Bagryansky, A. D. Khilchenko, A. N. Kvashnin, A. A. Lizunov, R. V. Voskoboynikov, A. L. Solomakhin, and H. R. Koslowski (TEXTOR team), *Review of Scientific Instruments*, **77** (2006) 053501.
- [6] S. Ya. Tochitsky, V. O. Petukhov, V. A. Gorobets, V. V. Churakov, V. N. Jakimovich,, *Applied Optics*, **36** (1997), 1882.

FIGURE CAPTIONS

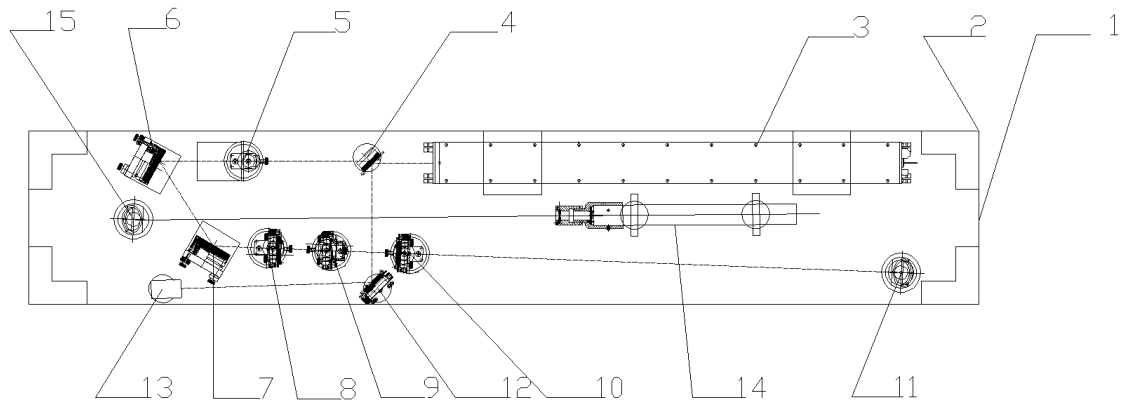


Figure 1. Layout of the “laser level” of SIMDI: 1 – optical breadboard (solid aluminum, 1640x300x19 mm), 2 – bearing to mount module in the special support holder structure, 3 – SYNRAD CO₂ laser, 4 – beam splitter plate, 5 – electromagnetic beam shutter, 6, 7 – plane mirror, 8, 10 – lens, 9 – aperture, 11 – periscope mirror, 12 – beam splitter plate, 13 – beam power monitor, 14 – alignment He-Ne laser with the beam expander telescope, 15 – He-Ne periscope mirror

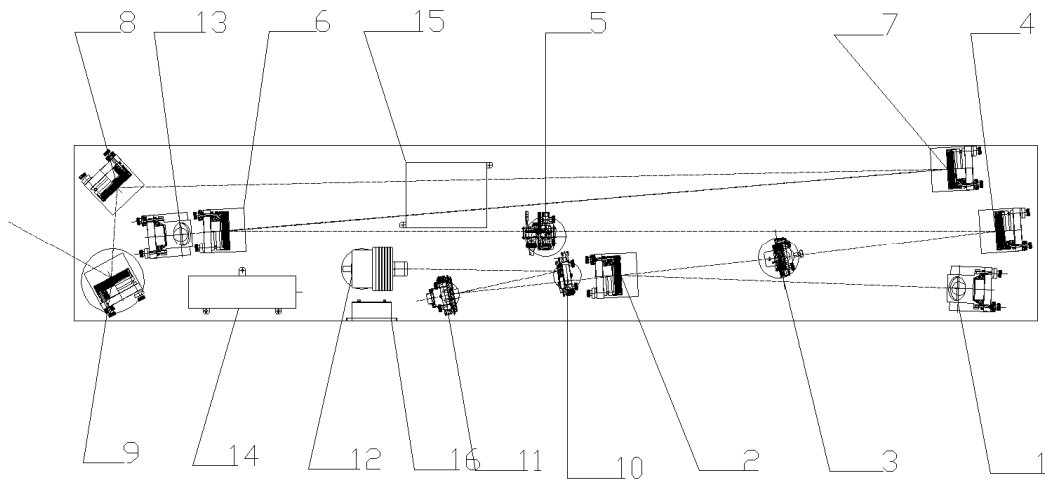


Figure 2. Layout of the “optical level”: 1 – periscope head, 2 – spherical mirror, 3 – frequency doubler crystal in the holder, 4 – spherical mirror, 5 – electro-optical cell in the holder, 6 – plane mirror for He-Ne and CO₂ beam alignment, 7 – spherical mirror, 8 – plane mirror, 9 – plane terminal mirror, 10 – plane mirror, 11 – spherical mirror combined with the beam position monitor, 12 – main photodetector, 13 – periscope head for He-Ne laser, 14-16 – electronic modules

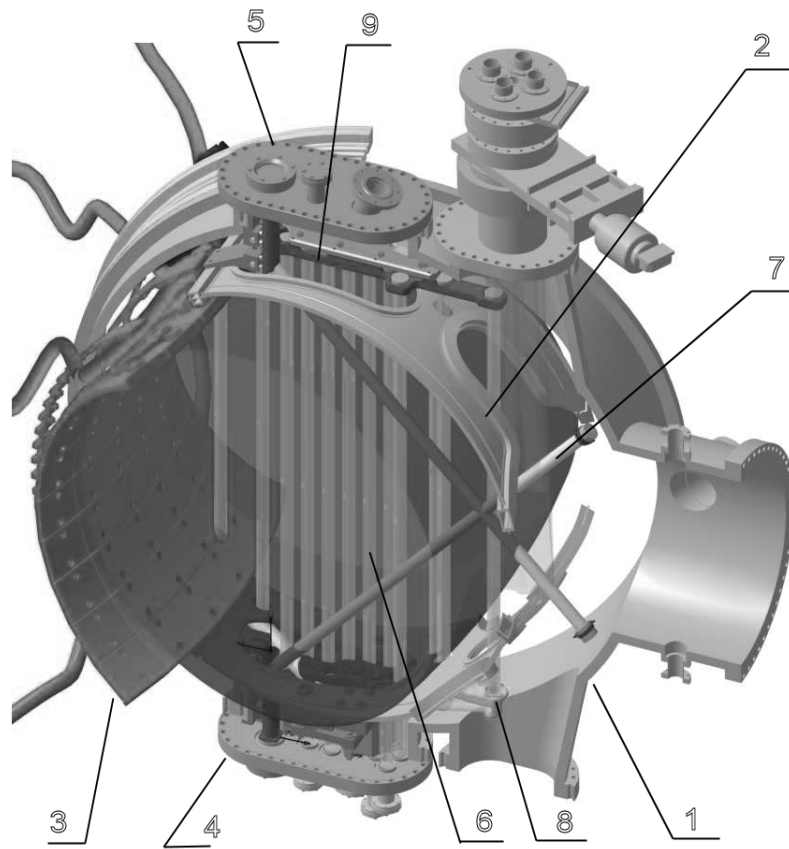


Figure 3. Layout of 14-channel measurement pattern: 1 – TEXTOR vacuum vessel, 2 – segment of liner, 3 – segment of Dynamic Ergodic Divertor of TEXTOR tokamak, 4 – lower diagnostic port, 5 – upper diagnostic port, 6 – vertical probing beam, 7 – diagonal probing beam, 8 – part of in-vessel mirror structure, 9 – retroreflector holder structure.

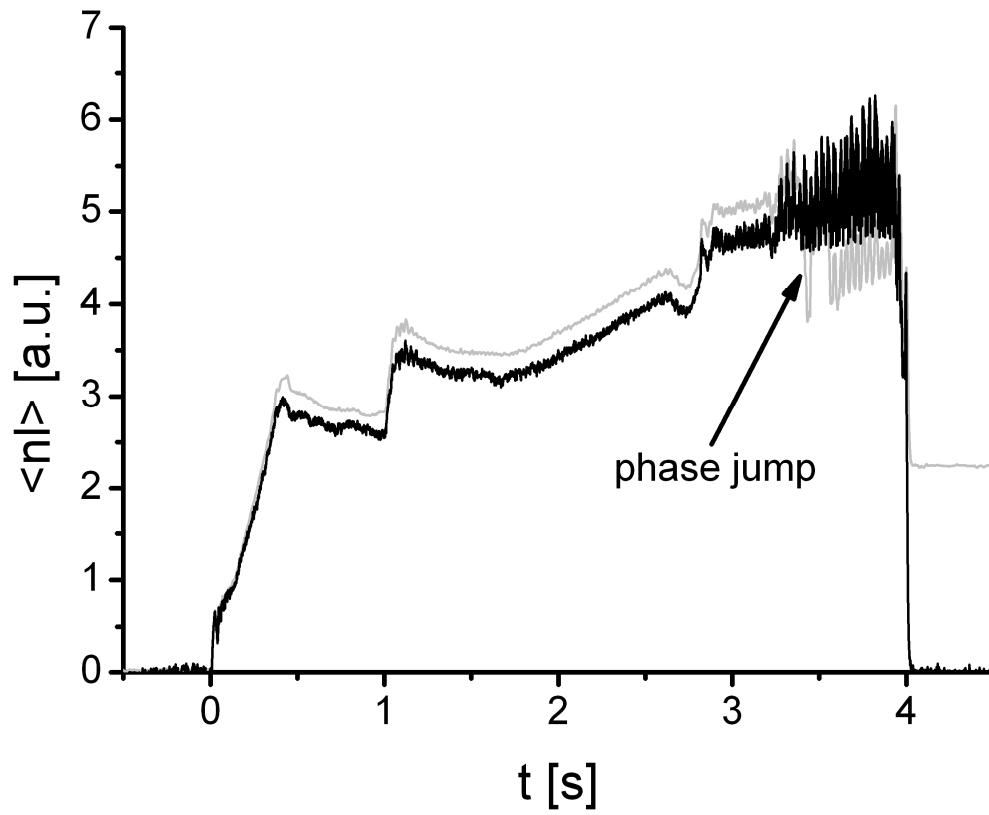


Figure 4. Plot of plasma line-integrated density: Black curve - signal acquired by dispersion interferometer prototype; grey curve – signal acquired by HCN interferometer in TEXTOR discharge #104337. Plasma density control was performed by DI.

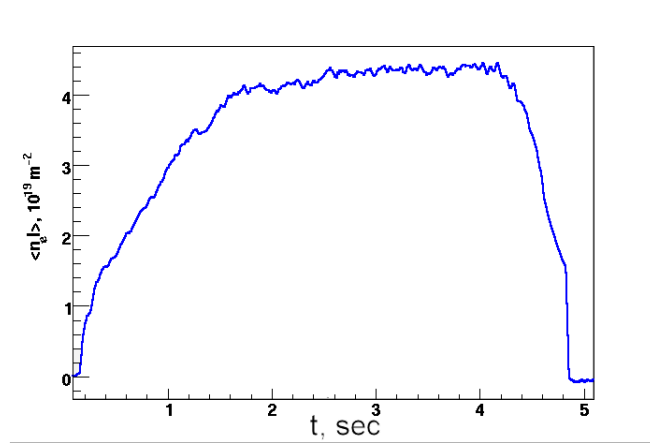


Figure 5: Plot of plasma line-integrated density acquired by dispersion interferometer module (SIMDI) during commissioning in TEXTOR discharge #107396.